Nonergodic Measurements of Qubit Frequency Noise

Filip Wudarski,[1] Yaxing Zhang,[2] and M. I. Dykman[3]
[1]USRA Research Institute for Advanced Computer Science (RIACS), Mountain View, California 94043, USA
[2]Google Quantum AI, Santa Barbara, California 93111, USA
[3]Department of Physics and Astronomy, Michigan State University, East Lansing, Michigan 48824, USA

(Received 10 May 2023; revised 26 September 2023; accepted 13 November 2023; published 6 December 2023)

Slow fluctuations of a qubit frequency are one of the major problems faced by quantum computers. To understand their origin it is necessary to go beyond the analysis of their spectra. We show that characteristic features of the fluctuations can be revealed using comparatively short sequences of periodically repeated Ramsey measurements, with the sequence duration smaller than needed for the noise to approach the ergodic limit. The outcomes distribution and its dependence on the sequence duration are sensitive to the nature of the noise. The time needed for quantum measurements to display quasiergodic behavior can strongly depend on the measurement parameters.

DOI: 10.1103/PhysRevLett.131.230201

Introduction.—Because of the probabilistic nature of quantum measurements, many currently implemented quantum algorithms rely on repeatedly running a quantum computer. It is important that the qubit parameters remain essentially the same between the runs. This imposes a constraint on comparatively slow fluctuations of the qubit parameters, in particular qubit frequencies, and on developing means of revealing and charactetizing such fluctuations.

Slow qubit frequency fluctuations have been a subject of intense studies [1–25]. Of primary interest has been their spectrum, although their statistics has also attracted interest [26–36]. This statistics may help to reveal the source of the underlying noise. In particular, fluctuations from the coupling to a few two-level systems (TLSs) should be non-Gaussian [27,32,37–43]. They are particularly important for solid state-based qubits, including those based on Josephson junctions and spin and charge states in semiconductors. Fluctuation statistics has been often described in terms of higher-order time correlators. Most work thus far has been done on fluctuations with the correlation time smaller than the qubit decay time.

Here we show that important information about qubit frequency fluctuations can be extracted from what we call nonergodic measurements. The idea is to perform M successive qubit measurements over time longer than the qubit decay time but shorter than the noise correlation time. The measurement outcomes are determined by the instantaneous state of the noise source, for example, by the instantaneous TLSs' states. They vary from one series of M measurements to another. Thus the outcome distribution reflects the distribution of the noise source over its states. It provides information that is washed out in the ensemble averaging inherent to ergodic measurements.

Closely related is the question of how long should a quantum measurement sequence be in order to reach the ergodic limit. Does the measurement duration depend on the type and parameters of the measurement, not only the noise source properties, and if so, on which parameters?

A convenient and frequently used method of performing successive measurements is to repeat them periodically. In this case the duration of data acquisition of M measurements is $\propto M$. For the measurements to be nonergodic it should suffice for this duration to be smaller than the noise correlation time. This imposes a limitation on M from above. The limitation on M from below is imposed by the uncertainty that comes from the quantum nature of the measurements.

We consider a periodic sequence of Ramsey measurements sketched in Fig. 1. At the beginning of a measurement, the qubit, initially in the ground state $|0\rangle$, is rotated about the y axis of the Bloch sphere by $\pi/2$, which brings it to the state $(|0\rangle + |1\rangle)/\sqrt{2}$. After time t_R the rotation is repeated and is followed by a projective measurement of finding the qubit in state $|1\rangle$. The qubit is then reset to $|0\rangle$, cf. [44]. In our scheme the measurements are repeated $M \gg 1$ times, with period $t_{\rm cyc}$.

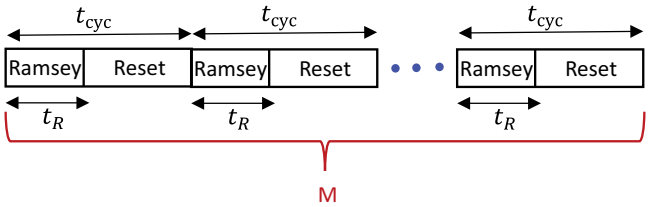

FIG. 1. Schematics of M Ramsey measurements. In each measurement the qubit phase is accumulated over time t_R. The measurements give the probability p to find the qubit in state $|1\rangle$. After a measurement the qubit is reset to state $|0\rangle$. The measurements are repeated with period $t_{\rm cyc}$.

The outcome of a kth Ramsey measurement x_k is 0 or 1. The probability p to find $x_k = 1$ is determined by the qubit phase accumulated over time t_R. This phase comes from the detuning of the qubit frequency from the frequency of the reference drive and from the noise-induced qubit frequency fluctuations $\delta\omega_q(t)$. The detuning is controllable, and we will use ϕ_R to indicate the phase that comes from it. The Hamiltonian H_{fl} that describes frequency fluctuations and the phase θ_k accumulated in the kth measurement due to these fluctuations have the form

$$H_{fl} = -\frac{1}{2}\delta\omega_q(t)\sigma_z, \quad \theta_k = \int_{kt_{cyc}}^{kt_{cyc}+t_R} \delta\omega_q(t)dt \qquad (1)$$

(we set $\hbar = 1$); we associate the Pauli operators $\sigma_{x,y,z}$ with the operators acting on the qubit states. We are interested in slow frequency fluctuations. The correlation time of $\delta\omega_q(t)$ is $\gtrsim t_{cyc}$.

In terms of the phases θ and ϕ_R, the probability to have $x_k = 1$ is [45]

$$p(\theta) = \frac{1}{2}\left[1 + e^{-t_R/T_2}\cos(\phi_R + \theta)\right], \qquad (2)$$

where T_2^{-1} is the qubit decoherence rate due to fast processes leading to decay and dephasing. In the absence of qubit frequency noise $\theta = 0$ for all M measurements and the distribution of the measurement outcomes is a binomial distribution [46]. Because of the frequency noise, the phase θ in Eq. (2) becomes random, and thus the probability $p(\theta)$ also becomes random. The outcomes distribution is determined by the distribution of the values of θ. The sensitivity of $p(\theta)$ to θ is reduced by errors in the Ramsey gates, the preparation of the state $|0\rangle$, and the readout errors [47]. However, these errors are small. Moreover, they do not change the qualitative features of nonergodic measurements.

The randomness of the phase is captured by the probability $\rho(m|M)$ to have $x_k = 1$ as a measurement outcome m times in M measurements, $\rho(m|M) = \mathrm{Prob}(\sum_{k=1}^{M} x_k = m)$. We consider $\rho(m|M)$ for periodically repeated measurements, see Fig. 1. If the frequency noise has correlation time small compared to the period t_{cyc}, the phases θ_k in successive measurements are uncorrelated. Then $\rho(m|M)$ is still given by a binomial distribution,

$$\rho_{binom}(m|M) = \binom{M}{m} r_1^m (1 - r_1)^{M-m}, \qquad (3)$$

where $r_1 \equiv \langle x_k\rangle = \langle p(\theta)\rangle_\theta$; here $\langle\ldots\rangle_\theta$ indicates averaging over realizations of θ. For large M this distribution is close to a Gaussian peak centered at r_1.

We are interested in the opposite case of slow frequency noise. Here the distribution $\rho(m|M)$ can strongly deviate from the binomial distribution. The deviation becomes pronounced and characteristic of the noise if Mt_{cyc} is comparable or smaller than the noise correlation time while M is still large.

The effect is particularly clear in the *static limit*, where the noise does not change over time Mt_{cyc}, i.e., the phase θ remains constant during M measurements. Even though θ is constant, its value $\theta = \theta(\ell)$ is random, it varies from one series of M measurements to another. Here ℓ enumerates the possible discrete values of θ, which are determined, for example, by the states of the TLSs, and we assume that noise correlations decay between successive series. The probability $P[\theta(\ell)]$ to have a given $\theta(\ell)$ is determined by the noise statistics. The distribution of the outcomes $\rho(m|M)$ is obtained by averaging the results of multiple repeated series of M measurements. Extending the familiar arguments that lead to Eq. (3), we find

$$\rho(m|M) = \binom{M}{m}\sum_{\ell} P[\theta(\ell)]p^m[\theta(\ell)] \times \{1 - p[\theta(\ell)]\}^{M-m}. \qquad (4)$$

The distribution (4) directly reflects the distribution of the noise over its states. In particular, if the values of $\theta(\ell)$ are discrete and well separated (see an example below), $\rho(m|M)$ has a characteristic fine structure with peaks located at $m \approx Mp[\theta(\ell))]$ for $M \gg 1$; the peak heights are determined by $P[\theta(\ell)]$.

An important example of slow frequency noise is the noise that results from dispersive coupling to a set of slowly switching TLSs,

$$\delta\hat{\omega}_q(t) = \sum_n V^{(n)}(\hat{\tau}_z^{(n)} - \langle\hat{\tau}_z^{(n)}\rangle). \qquad (5)$$

Here $n = 1, \ldots, N_{TLS}$ enumerates the TLSs, $\hat{\tau}_z^{(n)}$ is the Pauli operator of the nth TLS, $\langle\hat{\tau}_z^{(n)}\rangle$ is its average value, and $V^{(n)}$ is the coupling parameter; the states of the nth TLS are $|0\rangle^{(n)}$ and $|1\rangle^{(n)}$, and $\hat{\tau}_z^{(n)}|i\rangle^{(n)} = (-1)^i|i\rangle^{(n)}$ with $i = 0, 1$. We assume that the TLSs do not interact with each other. Their dynamics is described by the balance equations for the state populations. The only parameters are the rates $W_{ij}^{(n)}$ of $|i\rangle^{(n)} \to |j\rangle^{(n)}$ transitions, where $i, j = 0, 1$ [48].

The rates $W_{ij}^{(n)}$ give the stationary occupations of the TLSs states $w_{0,1}^{(n)}$, with $w_0^{(n)} = W_{10}^{(n)}/W^{(n)}$, $w_1^{(n)} = 1 - w_0^{(n)}$. Parameter $W^{(n)} = W_{01}^{(n)} + W_{10}^{(n)}$ is the TLS relaxation rate. The value of $\min W^{(n)}$ gives the reciprocal correlation time of the noise from the TLSs. We disregard the effect of the qubit on the TLSs dynamics, including measurements and resets, assuming that the TLSs decoherence rates are much larger than $V^{(n)}$. This is a good approximation for low-frequency TLSs coupled to solid-state based qubits.

In the static-limit approximation, the TLSs remain in the initially occupied states $|0\rangle^{(n)}$ or $|1\rangle^{(n)}$ during all M measurements. Then, from Eq. (5), the phase that the qubit accumulates during a measurement (before subtracting the average accumulated phase) is $\theta(\{j_n\}) = \sum_n (-1)^{j_n} V^{(n)} t_R$. Here $j_n = 0$ if the occupied TLS state is $|0\rangle^{(n)}$ and $j_n = 1$ if the occupied state is $|1\rangle^{(n)}$. The probability to have a given $\theta(\{j_n\})$ is determined by the stationary state occupations, $P[\theta(\{j_n\})] = \prod_n w_{j_n}^{(n)}$.

For the TLSs' induced noise, ℓ in Eq. (4) enumerates various combinations $\{j_n\}$. With the increasing coupling $V^{(n)}$, the separation of the values of $\theta(\{j_n\})$ increases, helping to observe the fine structure of $\rho(m|M)$.

The expression for $\rho(m|M)$ simplifies in the important case where the TLSs are symmetric, $w_0^{(n)} = w_1^{(n)} = 1/2$, and all coupling parameters are the same, $V^{(n)} = V$, cf. [2,10]. In this case $\theta(\{j_n\})$ takes on values $\theta_{\rm sym}(\ell) = Vt_R(2\ell - N_{\rm TLS})$ with $0 \le \ell \le N_{\rm TLS}$, and

$$\rho(m|M) = 2^{-N_{\rm TLS}} \binom{M}{m} \sum_{\ell} \binom{N_{\rm TLS}}{\ell} p^m[\theta_{\rm sym}(\ell)] \times \{1 - p[\theta_{\rm sym}(\ell)]\}^{M-m}. \quad (6)$$

The phases $\theta_{\rm sym}(\ell)$ are determined by the coupling constant V multiplied by the difference of the number of TLSs in the states $|0\rangle$ and $|1\rangle$, so that $\theta_{\rm sym}(\ell)$ may be significantly larger than for a single TLS [47].

The probability $\rho(m|M)$ of having "1" m times in M measurements has a characteristic form also in the case of Gaussian frequency noise if the noise is slow, so that $\delta\omega_{\rm q}(t)$ does not change over time $Mt_{\rm cyc}$. An important example of slow noise is $1/f$ noise. In the static limit $\rho(m|M)$ is described by an extension of Eq. (4), which takes into account that θ takes on continuous values. Respectively, one has to change in Eq. (4) from the sum over ℓ to the integral over $\theta(\ell)$, with $P[\theta(\ell)]$ becoming the probability density. For Gaussian noise $P[\theta(\ell)] = (2\pi f_0)^{-1/2} \exp[-\theta^2(\ell)/2f_0]$, where $f_0 = \langle \delta\omega_{\rm q}^2 \rangle t_R^2$ (we assume that $\langle \delta\omega_{\rm q} \rangle = 0$). The distribution $\rho(m|M)$ does not have fine structure; it depends only on the noise intensity in the static limit.

The opposite of the static limit is the ergodic limit, where $Mt_{\rm cyc}$ is much larger than the noise correlation time and the noise has time to explore all states during the measurements. In this limit $\rho(m|M)$ as a function of m/M has a narrow peak at $r_1 = \langle m/M \rangle \equiv \sum_m (m/M)\rho(m|M)$, with $\langle [(m/M) - r_1]^n \rangle \propto M^{-n/2}$ for even n.

Simulations.—We performed numerical simulations to explore the transition from the static to the ergodic limit and the features of $\rho(m|M)$ for slow noise. Here we present the results for $t_{\rm cyc} = 3t_R$. This ratio can be easily implemented in experiment. For example, for transmons a limit imposed by decay and fast dephasing is $t_R \lesssim 0.3$ ms, whereas the gate duration is $\lesssim$25 ns and the reset time can be $\lesssim$0.5 μs [49–51]. Choosing $t_{\rm cyc}$ of order of a few t_R allows applying the results to the noise in the kilohertz range, which plays an important role in transmons. The simulations were repeated at least 10^5 times. In Fig. 2 we show $\rho(m|M)$ for the noise from symmetric TLSs, $W_{01}^{(n)} = W_{10}^{(n)} = W^{(n)}/2$ (see [47] for other $t_{\rm cyc}/t_R$ and for the results on asymmetric TLSs).

Figure 2 shows evolution of $\rho(m|M)$ with the varying measurements number M. It is very different for different numbers of TLSs and the measurement parameter ϕ_R. The figure refers to a relatively weak qubit-TLS coupling. Panel (a) refers to a single TLS. Here, in the static limit

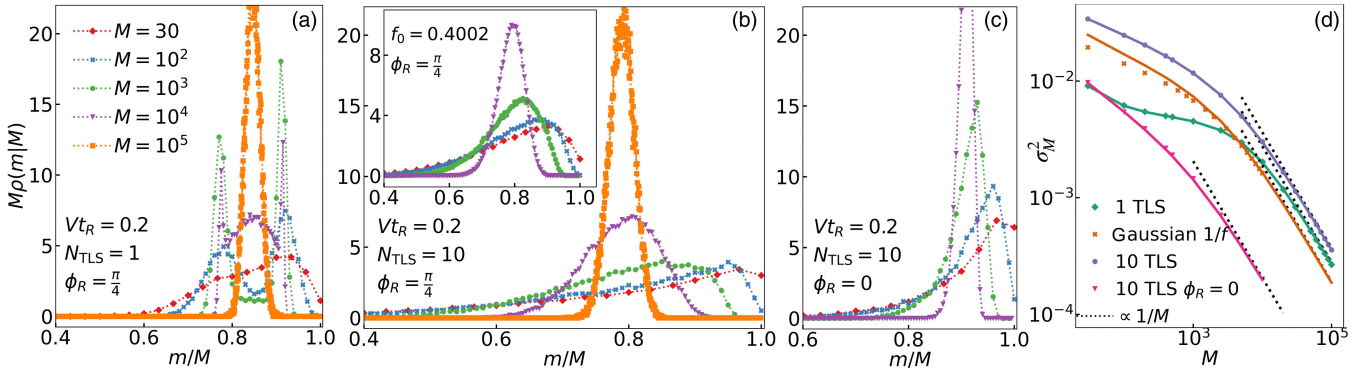

FIG. 2. Transition from nonergodic to ergodic behavior with the increasing number of measurements. Red diamonds, blue crosses, green dots, purple triangles, and orange squares in panels (a)–(c) show $\rho(m|M)$ for $M = 30, 10^2, 10^3, 10^4$, and 10^5, respectively. The scaled parameter of the dispersive qubit-to-TLS coupling is $Vt_R = 0.2$. The control parameter ϕ_R is $\pi/4$ in (a) and (b). (a) Coupling to a single symmetric TLS with the scaled switching rate $Wt_R = 1.2 \times 10^{-4}$. (b) Coupling to 10 symmetric TLSs with the switching rates $W^{(n)}t_R = \exp(-3n/4)$, $n = 3, 4, \ldots, 12$. The inset shows the results for Gaussian $1/f$-type noise described in the text, $f_0 = \langle \delta\omega_q^2 \rangle t_R^2$. (c) Coupling to the same 10 TLSs as in panel (b), but for $\phi_R = 0$. (d) Variance of $\rho(m|M)$ for the data in panels (a)–(c); solid lines show the theory; data points show the results of the simulations; dashed lines show the ergodic limit.

$\rho(m|M)$ is double peaked, with the peaks at $m/M \approx 0.92$ and 0.78, from Eq. (6). Such peaks are seen for $M = 10^2$, 10^3, and 10^4, where $MWt_{\rm cyc}$ varies from 0.036 to 3.6, even though one might expect the system to be close to ergodic for $M = 10^4$. For $M = 30$ the fine structure is smeared, because M is not large enough to average out the uncertainty of quantum measurements, but $\rho(m|M)$ displays a significant and characteristic asymmetry. For $M = 10^5$, where $MWt_{\rm cyc} = 36$, the distribution does approach the ergodic limit, with a single peak at $m/M \approx 0.85$ [47].

Figure 2(b) refers to 10 TLSs. Their scaled switching rates $W^{(n)}t_{\rm cyc}$ form a geometric series, varying from ≈ 0.32 to $\approx 3.7 \times 10^{-4}$. The power spectrum of the noise $\delta\omega_q(t)$ is close to $1/f$ in a broad frequency range for such form of $W^{(n)}$ [47]. However, for the chosen $W^{(n)}t_{\rm cyc}$ the static limit does not apply and the fine structure is not resolved. The asymmetry of $\rho(m|M)$ is profound. It gradually decreases with the increasing M. It is important that, for $\phi_R = \pi/4$, the distribution approaches the ergodic limit for $Mt_{\rm cyc} \times (\min W^{(n)}) \gtrsim 30$, similar to the case of one TLS (the choice $\phi_R = \pi/4$ is explained in [47]).

For comparison, the inset in Fig. 2(b) shows the evolution of $\rho(m|M)$ for $1/f$-type Gaussian frequency noise $\delta\omega_{\rm q}(t)$ with the power spectrum $S_q(\omega) = (2D/\pi)\int_{\omega_{\rm min}}^{\infty} dW/(W^2+\omega^2)$. The cutoff frequency $\omega_{\rm min}$ is set equal to the minimal switching rate of the 10 TLSs in the main panel $\min(W^{(n)})$, and the intensity D is chosen so that, in the ergodic limit, $\rho(m|M)$ has a maximum for the same m/M as for the 10 TLSs.

The result of Fig. 2(c) is surprising. The data refers to the same 10 TLSs as in panel (b), except that the phase of the Ramsey measurement is set to $\phi_R = 0$. The change of ϕ_R does not affect the dynamics of the TLSs. However, for the same M values, the peak of $\rho(m|M)$ is much narrower than for $\phi_R = \pi/4$ and $\rho(m|M)$ approaches the ergodic limit for an order of magnitude smaller M.

A simple measure of closeness of $\rho(m|M)$ to the ergodic limit is the variance $\sigma_M^2 = \sum_m (m/M)^2\rho(m|M) - r_1^2$, where $r_1 = \langle x_k \rangle$. It is expressed in terms of the pair correlator of x_k [47]. In the ergodic limit $\sigma_M^2 \propto M^{-1}$, but its value depends on the noise correlation. Figure 2(d) shows how σ_M^2 approaches the ergodic scaling [52]. For $\phi_R = \pi/4$ and the same correlation time of the noise from 1 or 10 TLSs and of Gaussian noise ($\sim 1/\min W^{(n)}$ and $\sim 1/\omega_{\rm min}$), σ_M^2 behaves similarly for large M. Yet, for the same 10 TLSs, but for $\phi_R = 0$ the variance approaches the ergodic limit much faster.

The fine structure of $\rho(m|M)$ is more pronounced for larger scaled coupling $|V|t_R$. For example, for one TLS the interpeak distance is $\approx \sin(Vt_R)\sin\phi_R$. It is important that the coupling parameter Vt_R can be changed in the experiment by varying t_R. The ratio between $Mt_{\rm cyc}$ and the noise correlation time can be changed, too, and not only by varying M (which affects the statistics), but also by varying $t_{\rm cyc}$. The fine structure is more pronounced for smaller $t_{\rm cyc}$ [47].

In a qualitative distinction from the power spectrum of the frequency noise, which has the same form for a symmetric and an asymmetric TLS, $\rho(m|M)$ sensitively depends on the TLS asymmetry. In particular, $\rho(m|M) = \rho(M-m|M)$ for $\phi_R = \pi/2$ for symmetric TLSs, whereas for asymmetric TLSs $\rho(m|M) \neq \rho(M-m|M)$; the fine structure is also better resolved for $\phi_R = \pi/2$ [47]. This shows that nonergodic measurements can be used to characterize the coupling to low-frequency TLSs, where the standard technique of tuning a qubit in resonance with a TLS does not apply.

The presence of a characteristic fine structure of $\rho(m|M)$ is an unambiguous indication of the noise coming from the coupling to slow TLSs. Observing it would be a long-sought direct proof of the nature of the low-frequency noise, which was early on associated with, but not directly proved to be caused by, TLSs [2]. For large $N_{\rm TLS}$ it becomes more complicated to characterize individual TLSs using $\rho(m|M)$ as the peaks of $\rho(m|M)$ start overlapping. However, for small $N_{\rm TLS} \lesssim 5$ our simulations show that the number of peaks of the fine structure and their amplitudes and shapes still enable estimating the number and the parameters of slow TLSs.

For 10 TLSs, as seen in panel (b), the distribution is broad and strongly asymmetric. Both its shape and the position of the maximum sensitively depend on the coupling. We note the distinction from direct measurements of qubit frequency as a function of time [3,6,21], which is efficient for still much slower noise.

Nonergodic measurements are more revealing in terms of the mechanism of low-frequency noise than the ergodic ones [52], particularly where the fine structure is pronounced. In addition to t_R, $t_{\rm cyc}$, and ϕ_R, they have M as an important control parameter. However, the two methods complement each other. Besides the TLSs, nonergodic measurements can be used to study other low-frequency noise sources, such as the noise from photons in a superconducting cavity and from nuclear spins in electron spin based qubits.

Discussion of ergodicity.—To reach ergodic limit, a system of 10 TLSs has to visit its 2^{10} states. The needed time is a property of the TLSs themselves. However, the results of the measurements can approach a quasiergodic limit, except for the far tail of the outcomes distribution, over a shorter time. This time depends on the correlation time of the fluctuations relevant for the measurement, but this correlation time is not obvious in advance. In our setup, the noise is "measured" by the qubit, and then the results are read through Ramsey measurements. As we show, an important parameter is the qubit-to-TLSs coupling, which we chose to be the same for all TLSs to avoid any bias. Unexpectedly, there is another important parameter, the phase ϕ_R.

The effect of ϕ_R on the convergence to the ergodic limit is not obvious in advance. It is seen already in the dependence on ϕ_R of the centered correlator $\tilde{r}_2(k)$ of the measurement outcomes. For weak coupling to slowly switching TLSs, $V^{(n)}t_R \ll 1$ and $W^{(n)}t_R \ll 1$, and for $|\phi_R| \ll 1$ this correlator is small. Moreover, it falls off with the increasing k much faster than for $\phi_R = \mathcal{O}(1)$ [47]. This indicates a reduced role of slow noise correlations for small ϕ_R. Respectively, the ergodic limit is reached much faster with the increasing M.

Conclusions.—We studied the distribution of the outcomes of periodically repeated Ramsey measurements with the sequence length Mt_{cyc} shorter than needed to approach the ergodic limit. Such distribution proves to provide an alternative, and sensitive, means of characterizing qubit frequency noise with a long correlation time. In contrast to bi- or trispectra, such distribution incorporates noise correlators of order $M \gg 1$. The analytical results and simulations show that, for non-Gaussian noise, in particular the noise from TLSs, the distribution can display a characteristic fine structure. Even where there is no fine structure, the form of the distribution and its evolution with the sequence length are noise specific.

The results show that the way the system approaches the ergodic limit with the increasing number of quantum measurements depends not only on the noise source but also on the character and parameters of the measurement. These parameters are not necessarily known in advance. Their effect can be strong and depends on the noise source. Measurement outcomes can practically approach the ergodic limit well before the noise source approaches this limit.

F. W. and M. I. D. acknowledge partial support from NASA Contract No. NNA16BD14C, and from Google under NASA-Google SAA2-403512.

[1] Y. Nakamura, Yu. A. Pashkin, T. Yamamoto, and J. S. Tsai, Charge echo in a Cooper-pair box, Phys. Rev. Lett. **88**, 047901 (2002).
[2] G. Ithier, E. Collin, P. Joyez, P. J. Meeson, D. Vion, D. Esteve, F. Chiarello, A. Shnirman, Y. Makhlin, J. Schriefl, and G. Schön, Decoherence in a superconducting quantum bit circuit, Phys. Rev. B **72**, 134519 (2005).
[3] R. C. Bialczak, R. McDermott, M. Ansmann, M. Hofheinz, N. Katz, E. Lucero, M. Neeley, A. D. O'Connell, H. Wang, A. N. Cleland, and J. M. Martinis, $1/f$ flux noise in Josephson phase qubits, Phys. Rev. Lett. **99**, 187006 (2007).
[4] G. A. Álvarez and D. Suter, Measuring the spectrum of colored noise by dynamical decoupling, Phys. Rev. Lett. **107**, 230501 (2011).
[5] J. Bylander, S. Gustavsson, F. Yan, F. Yoshihara, K. Harrabi, G. Fitch, D. G. Cory, Y. Nakamura, J.-S. Tsai, and W. D. Oliver, Noise spectroscopy through dynamical decoupling with a superconducting flux qubit, Nat. Phys. **7**, 565 (2011).
[6] D. Sank, R. Barends, R. C. Bialczak, Y. Chen, J. Kelly, M. Lenander, E. Lucero, M. Mariantoni, A. Megrant, M. Neeley, P. J. J. O'Malley, A. Vainsencher, H. Wang, J. Wenner, T. C. White, T. Yamamoto, Y. Yin, A. N. Cleland, and J. M. Martinis, Flux noise probed with real time qubit tomography in a Josephson phase qubit, Phys. Rev. Lett. **109**, 067001 (2012).
[7] F. Yan, J. Bylander, S. Gustavsson, F. Yoshihara, K. Harrabi, D. G. Cory, T. P. Orlando, Y. Nakamura, J.-S. Tsai, and W. D. Oliver, Spectroscopy of low-frequency noise and its temperature dependence in a superconducting qubit, Phys. Rev. B **85**, 174521 (2012).
[8] K. C. Young and K. B. Whaley, Qubits as spectrometers of dephasing noise, Phys. Rev. A **86**, 012314 (2012).
[9] G. A. Paz-Silva and L. Viola, General transfer-function approach to noise filtering in open-loop quantum control, Phys. Rev. Lett. **113**, 250501 (2014).
[10] F. Yoshihara, Y. Nakamura, F. Yan, S. Gustavsson, J. Bylander, W. D. Oliver, and J.-S. Tsai, Flux qubit noise spectroscopy using Rabi oscillations under strong driving conditions, Phys. Rev. B **89**, 020503(R) (2014).
[11] M. Kim, H. J. Mamin, M. H. Sherwood, K. Ohno, D. D. Awschalom, and D. Rugar, Decoherence of near-surface nitrogen-vacancy centers due to electric field noise, Phys. Rev. Lett. **115**, 087602 (2015).
[12] M. Brownnutt, M. Kumph, P. Rabl, and R. Blatt, Ion-trap measurements of electric-field noise near surfaces, Rev. Mod. Phys. **87**, 1419 (2015).
[13] P. J. J. O'Malley *et al.*, Qubit metrology of ultralow phase noise using randomized benchmarking, Phys. Rev. Appl. **3**, 044009 (2015).
[14] F. Yan, S. Gustavsson, A. Kamal, J. Birenbaum, A. P. Sears, D. Hover, T. J. Gudmundsen, D. Rosenberg, G. Samach, S. Weber, J. L. Yoder, T. P. Orlando, J. Clarke, A. J. Kerman, and W. D. Oliver, The flux qubit revisited to enhance coherence and reproducibility, Nat. Commun. **7**, 1 (2016).
[15] B. A. Myers, A. Ariyaratne, and A. C. B. Jayich, Double-quantum spin-relaxation limits to coherence of near-surface nitrogen-vacancy centers, Phys. Rev. Lett. **118**, 197201 (2017).
[16] C. M. Quintana *et al.*, Observation of classical-quantum crossover of $1/f$ flux noise and its paramagnetic temperature dependence, Phys. Rev. Lett. **118**, 057702 (2017).
[17] G. A. Paz-Silva, L. M. Norris, and L. Viola, Multiqubit spectroscopy of Gaussian quantum noise, Phys. Rev. A **95**, 022121 (2017).
[18] C. Ferrie, C. Granade, G. Paz-Silva, and H. M. Wiseman, Bayesian quantum noise spectroscopy, New J. Phys. **20**, 123005 (2018).
[19] C. Noel, M. Berlin-Udi, C. Matthiesen, J. Yu, Y. Zhou, V. Lordi, and H. Häffner, Electric-field noise from thermally activated fluctuators in a surface ion trap, Phys. Rev. A **99**, 063427 (2019).
[20] U. von Lüpke, F. Beaudoin, L. M. Norris, Y. Sung, R. Winik, J. Y. Qiu, M. Kjaergaard, D. Kim, J. Yoder, S. Gustavsson, L. Viola, and W. D. Oliver, Two-qubit spectroscopy of spatiotemporally correlated quantum noise in superconducting qubits, PRX Quantum **1**, 010305 (2020).
[21] T. Proctor, M. Revelle, E. Nielsen, K. Rudinger, D. Lobser, P. Maunz, R. Blume-Kohout, and K. Young, Detecting and

tracking drift in quantum information processors, Nat. Commun. **11**, 5396 (2020).
[22] G. Wolfowicz, F. J. Heremans, C. P. Anderson, S. Kanai, H. Seo, A. Gali, G. Galli, and D. D. Awschalom, Qubit guidelines for solid-state spin defects, Nat. Rev. Mater. **6**, 906 (2021).
[23] Y.-X. Wang and A. A. Clerk, Intrinsic and induced quantum quenches for enhancing qubit-based quantum noise spectroscopy, Nat. Commun. **12**, 6528 (2021).
[24] G. Burkard, T. D. Ladd, A. Pan, J. M. Nichol, and J. R. Petta, Semiconductor spin qubits, Rev. Mod. Phys. **95**, 025003 (2023).
[25] S. Burgardt, S. B. Jäger, J. Feß, S. Hiebel, I. Schneider, and A. Widera, Measuring the environment of a Cs qubit with dynamical decoupling sequences, J. Phys. B **56**, 165501 (2023).
[26] F. Li, A. Saxena, D. Smith, and N. A. Sinitsyn, Higher-order spin noise statistics, New J. Phys. **15**, 113038 (2013).
[27] G. Ramon, Non-Gaussian signatures and collective effects in charge noise affecting a dynamically decoupled qubit, Phys. Rev. B **92**, 155422 (2015).
[28] L. M. Norris, G. A. Paz-Silva, and L. Viola, Qubit noise spectroscopy for non-Gaussian dephasing environments, Phys. Rev. Lett. **116**, 150503 (2016).
[29] N. A. Sinitsyn and Y. V. Pershin, The theory of spin noise spectroscopy: A review, Rep. Prog. Phys. **79**, 106501 (2016).
[30] P. Szańkowski, G. Ramon, J. Krzywda, D. Kwiatkowski, and L Cywiński, Environmental noise spectroscopy with qubits subjected to dynamical decoupling, J. Phys. Condens. Matter **29**, 333001 (2017).
[31] Y. Sung, F. Beaudoin, L. M. Norris, F. Yan, D. K. Kim, J. Y. Qiu, U. von Lüpke, J. L. Yoder, T. P. Orlando, S. Gustavsson, L. Viola, and W. D. Oliver, Non-Gaussian noise spectroscopy with a superconducting qubit sensor, Nat. Commun. **10**, 3715 (2019).
[32] G. Ramon, Trispectrum reconstruction of non-Gaussian noise, Phys. Rev. B **100**, 161302(R) (2019).
[33] J. J. Burnett, A. Bengtsson, M. Scigliuzzo, D. Niepce, M. Kudra, P. Delsing, and J. Bylander, Decoherence benchmarking of superconducting qubits, npj Quantum Inf. **5**, 1 (2019).
[34] F. Sakuldee and Ł. Cywiński, Relationship between subjecting the qubit to dynamical decoupling and to a sequence of projective measurements, Phys. Rev. A **101**, 042329 (2020).
[35] Y.-X. Wang and A. A. Clerk, Spectral characterization of non-Gaussian quantum noise: Keldysh approach and application to photon shot noise, Phys. Rev. Res. **2**, 033196 (2020).
[36] X. You, A. A. Clerk, and J. Koch, Positive- and negative-frequency noise from an ensemble of two-level fluctuators, Phys. Rev. Res. **3**, 013045 (2021).
[37] E. Paladino, L. Faoro, G. Falci, and R. Fazio, Decoherence and $1/f$ noise in Josephson qubits, Phys. Rev. Lett. **88**, 228304 (2002).
[38] Y. M. Galperin, B. L. Altshuler, and D. V. Shantsev, Low-frequency noise as a source of dephasing of a qubit, in *Fundamental Problems of Mesoscopic Physics*, edited by I. V. Lerner (Kluwer Academic Publishing, The Netherlands, 2004).
[39] L. Faoro and L. Viola, Dynamical suppression of $1/f$ noise processes in qubit systems, Phys. Rev. Lett. **92**, 117905 (2004).
[40] Y. M. Galperin, B. L. Altshuler, J. Bergli, and D. V. Shantsev, Non-Gaussian low-frequency noise as a source of qubit decoherence, Phys. Rev. Lett. **96**, 097009 (2006).
[41] E. Paladino, Y. M. Galperin, G. Falci, and B. L. Altshuler, $1/f$ noise: Implications for solid-state quantum information, Rev. Mod. Phys. **86**, 361 (2014).
[42] C. Müller, J. H. Cole, and J. Lisenfeld, Towards understanding two-level-systems in amorphous solids: Insights from quantum circuits, Rep. Prog. Phys. **82**, 124501 (2019).
[43] Z. Huang, X. You, U. Alyanak, A. Romanenko, A. Grassellino, and S. Zhu, High-order qubit dephasing at sweet spots by non-Gaussian fluctuators: Symmetry breaking and Floquet protection, Phys. Rev. Appl. **18**, L061001 (2022).
[44] T. Fink and H. Bluhm, Noise spectroscopy using correlations of single-shot qubit readout, Phys. Rev. Lett. **110**, 010403 (2013).
[45] M. A. Nielsen and I. L. Chuang, *Quantum Computation and Quantum Information: 10th Anniversary Edition* (Cambridge University Press, England, 2011).
[46] N. G. Van Kampen, *Stochastic Processes in Physics and Chemistry*, 3rd ed. (Elsevier, Amsterdam, 2007).
[47] See Supplemental Material at http://link.aps.org/supplemental/10.1103/PhysRevLett.131.230201 for more results on $\rho(m|M)$, including the fine structure, the effect of asymmetric TLSs, and the transition to the ergodic limit.
[48] P. W. Anderson, B. I. Halperin, and C. M. Varma, Anomalous low-temperature thermal properties of glasses and spin glasses, Philos. Mag. J. Theor. Exp. Appl. Phys. **25**, 1 (1972); W. A. Phillips, Tunneling states in amorphous solids, J. Low Temp. Phys. **7**, 351 (1972); W. A. Phillips, Two-level states in glasses, Rep. Prog. Phys. **50**, 1657 (1987).
[49] Google Quantum AI, Suppressing quantum errors by scaling a surface code logical qubit, Nature (London) **614**, 676 (2023).
[50] Y. Kim, A. Eddins, S. Anand, K. Wei, E. van den Berg, S. Rosenblatt, H. Nayfeh, Y. Wu, M. Zaletel, K. Temme, and A. Kandala, Evidence for the utility of quantum computing before fault tolerance, Nature (London) **618**, 1476 (2023).
[51] S. Krinner, N. Lacroix, A. Remm, A. D. Paolo, E. Genois, C. Leroux, C. Hellings, S. Lazar, F. Swiadek, J. Herrmann, G. J. Norris, C. K. Andersen, M. Müller, A. Blais, C. Eichler, and A. Wallraff, Realizing repeated quantum error correction in a distance-three surface code, Nature (London) **605**, 669 (2022).
[52] F. Wudarski, Y. Zhang, A. N. Korotkov, A. G. Petukhov, and M. I. Dykman, Characterizing low-frequency qubit noise, Phys. Rev. Appl. **19**, 064066 (2023).